BIOCHEMISTRY
including biophysical chemistry & molecular biology

Article

pubs.acs.org/biochemistry

Substrate Specificity of *Sphingobium chlorophenolicum* 2,6-Dichlorohydroquinone 1,2-Dioxygenase

Timothy E. Machonkin* and Amy E. Doerner

Department of Chemistry, Whitman College, 345 Boyer Avenue, Walla Walla, Washington 99362, United States

Supporting Information

ABSTRACT: PcpA is an aromatic ring-cleaving dioxygenase that is homologous to the well-characterized Fe(II)-dependent catechol extradiol dioxygenases. This enzyme catalyzes the oxidative cleavage of 2,6-dichlorohydroquinone in the catabolism of pentachlorophenol by *Sphingobium chlorophenolicum* ATCC 39723. ^{1}H NMR and steady-state kinetics were used to determine the regiospecificity of ring cleavage and the substrate specificity of the enzyme. PcpA exhibits a high degree of substrate specificity for 2,6-disubstituted hydroquinones, with halogens greatly preferred at those positions. Notably, the $k_{cat}^{app}/K_{mA}^{app}$ of 2,6-dichlorohydroquinone is ~40-fold higher than that of 2,6-dimethylhydroquinone. The asymmetric substrate 2-chloro-6-methylhydroquinone yields a mixture of 1,2- and 1,6-cleavage products. These two modes of cleavage have different $K_{mO_2}^{app}$ values (21 and 260 μM, respectively), consistent with a mechanism in which the substrate binds in two catalytically productive orientations. In contrast, monosubstituted hydroquinones show a limited amount of ring cleavage but rapidly inactivate the enzyme in an O_2-dependent fashion, suggesting that oxidation of the Fe(II) may be the cause. Potent inhibitors of PcpA include *ortho*-disubstituted phenols and 3-bromocatechol. 2,6-Dibromophenol is the strongest competitive inhibitor, consistent with PcpA's substrate specificity. Several factors that could yield this specificity for halogen substituents are discussed. Interestingly, 3-bromocatechol also inactivates the enzyme, while 2,6-dihalophenols do not, indicating a requirement for two hydroxyl groups for ring cleavage and for enzyme inactivation. These results provide mechanistic insights into the hydroquinone dioxygenases.

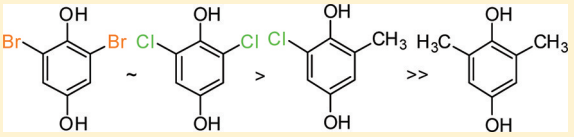

Bacteria use an astonishing range of molecules as carbon sources, a property that has been of interest for use in the bioremediation of xenobiotic compounds, including recalcitrant pollutants such as chlorinated organic compounds.[1−5] The study of these pollutant-degrading catabolic pathways has yielded a wealth of novel enzymes with interesting properties. The group of bacterial enzymes involved in the catabolism of aromatic hydrocarbons is one such example that has received considerable attention. In most cases, aerobic catabolism of aromatic hydrocarbons involves the oxidative ring cleavage of a catechol. The substrate specificity of these catechol dioxygenases can limit the range of aromatic hydrocarbons that can be utilized by a particular catabolic pathway, in part because of the buildup of toxic dead-end metabolites.[3] There are two types of catechol dioxygenases: the Fe(III)-dependent intradiol dioxygenases (IDOs), which cleave the C−C bond between the vicinal hydroxyl groups, and the Fe(II)-dependent extradiol dioxygenases (EDOs), which cleave the C−C bond adjacent to the vicinal hydroxyl groups.[6−10] Extensive studies of the EDOs using a range of experimental approaches (including structures of trapped intermediates) have yielded a generally accepted mechanism[6,7,10−12] supported by density functional theory calculations.[13,14]

In recent years, ring-cleaving dioxygenases that work on noncatecholic substrates, including salicylates and gentisates,[15−21] homogentisate,[22,23] 2-aminophenols,[24−27] and hydroquinones (that lack a carboxylate functional group), have been described.[28−34] All of these substrates consist of a hydroxyl-substituted aromatic ring with a hydroxyl, amino, or carboxylate at the *ortho* and/or *para* positions. Interestingly, all of these enzymes appear to share essentially the same type of metal-binding site employed by the EDOs: a single Fe(II) center bound to the protein by a 2-histidine-1-carboxylate facial-capping triad of ligands (or, in some cases, three histidines). This would seem to imply that the factors governing the substrate specificity among these ring-cleaving dioxygenases lie in the active site pocket and the second coordination sphere.

The dioxygenases that cleave hydroquinones lacking a carboxylate functional group [hydroquinone dioxygenases (HQDOs)] are unique among ring-cleaving dioxygenases in that their substrates cannot bind to the Fe(II) center in a bidentate fashion. However, they have been studied little, and only five have been reported to date. Three of these are homologues that are 40−50% identical in amino acid sequence: 2,6-dichlorohydroquinone 1,2-dioxygenase (PcpA) from the pentachlorophenol degradation pathway of *Sphingobium chlorophenolicum* ATCC 39723 (Scheme 1A),[28−30] chlorohydroquinone 1,2-dioxygenase (LinE) from the γ-hexachlorocyclohexane (lindane) degradation pathway of *Sphingobium japonicum* (formerly *Sphingomonas paucimobilis*) UT26 (Scheme 1B),[31] and MnpC, an HQDO from a putative

Received: June 2, 2011
Revised: August 23, 2011
Published: August 26, 2011

Scheme 1. Ring-Cleavage Reactions Catalyzed by the Known HQDOs

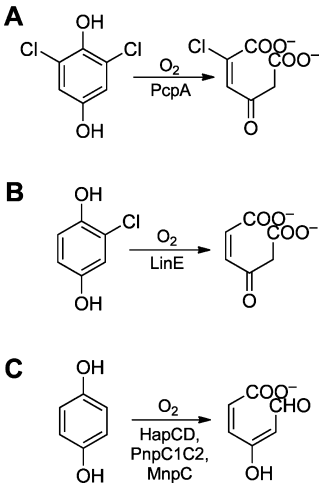

m-nitrophenol degradation pathway of *Cupriavidus necator* JMP134.[34] The two other HQDOs share no sequence identity with PcpA but are >60% identical in sequence with each other and cleave unsubstituted hydroquinone: HapCD from the 4-hydroxyacetophenone degradation pathway of *Pseudomonas fluorescens* ACB[32] and PnpC1C2 from the *p*-nitrophenol degradation pathway of *Pseudomonas putida* DLL-E4[33] (Scheme 1C). Thus, similar to the EDOs, which occur in two different classes (type I and type II),[8,9] there are two distinct structural classes of HQDOs. PcpA and its homologues (LinE and MnpC) and the type I EDOs are members of the "vicinal oxygen chelate" (VOC) superfamily, as first recognized by Xu et al.[29] However, our experimentally verified structural model of PcpA demonstrated that the four copies of the $\beta\alpha\beta\beta\beta\beta$ structural motif of the VOC superfamily are arranged differently in this enzyme and that residues His11, His227, and Glu276 are likely the ligands to the Fe(II) center.[35]

A remarkable property of PcpA and LinE is their ability to cleave chlorinated substrates. This contrasts with EDOs, which are known to be subjected to mechanism-based inactivation by chlorinated substrates.[36−39] However, whether PcpA and LinE exhibit an actual preference for chloro substituents or merely tolerate chloro substituents has not been previously established, because very little about the substrate specificity of these enzymes has been reported. Another HQDO, HapCD, has a higher activity with methylhydroquinone than it does for its native substrate, hydroquinone, and a lower activity toward chlorohydroquinone and other halogenated hydroquinones.[32] Understanding how a naturally occurring ring-cleaving dioxygenase can successfully utilize chlorinated substrates is an important area for study. Considerable effort has been spent in identifying EDOs capable of cleaving chlorinated substrates[39−46] and engineering EDOs with improved abilities to cleave chlorinated substrates and/or reduced sensitivity to inactivation;[47−50] however, success on the latter front has been limited.

In this work, we investigated the range of molecules that can act as substrates and inhibitors of PcpA, including structural variants of the physiological substrate (2,6-dichlorohydroquinone) and substrates of other ring-cleaving dioxygenases. Steady-state kinetic studies were used to establish the substrate specificity of the enzyme as well as the mode and strength of inhibition of various inhibitors. ^{1}H NMR was used to determine the regiospecificity of the enzyme and the tautomeric states of the cleavage products. The results provide insights into the mechanism of ring cleavage.

EXPERIMENTAL PROCEDURES

Protein Production. The expression and purification of PcpA were performed by the method of Xun and co-workers[30] with the modifications described previously.[35]

Preparation of Potential Substrates and Inhibitors. 2,6-Dibromobenzoquinone was synthesized by the method of Ungnade and Zilch.[51] The identity of this compound was confirmed by ^{1}H NMR ($CDCl_3$): δ 7.33 (s). 2-Chloro-6-methylhydroquinone was synthesized by the method of Burton and Prail, with the following additional purification steps.[52] The product of the first step (1,4-diacetoxy-2-chloro-6-methylbenzene) was purified by silica gel column chromatography. The identity of this compound was confirmed by ^{1}H NMR ($CDCl_3$): δ 6.99 (d, J = 2.2 Hz, 1H), 6.83 (d, J = 2.2 Hz, 1H), 2.30 (s, 3H), 2.22 (s, 3H), 2.13 (s, 3H). The final product was recrystallized from hot dichloromethane. The identity of the product was confirmed by ^{1}H NMR ($CDCl_3$): δ 6.71 (d, J = 2.8 Hz, 1H), 6.58 (d, J = 2.8 Hz, 1H), 2.26 (s, 3H). The purity of both compounds was determined to be >98% by both thin layer chromatography and ^{1}H NMR. Chlorobenzoquinone was purchased from Alfa Aesar and repurified by silica gel column chromatography. All other compounds were purchased commercially, were reagent grade, and were used without further purification.

Kinetic Studies. The rate of the enzymatic reaction was determined by measuring product formation by a spectrophotometric assay developed by Xun and co-workers[30] with the modification (addition of imidazole) described previously.[35] The assay was performed on a Cary 50 Bio or Cary 5000 (for the O_2 dependence experiments) UV−visible spectrophotometer (Varian). In some cases, the hydroquinones were formed by in situ reduction of the substituted benzoquinone with $NaBH_4$. This was done with 2,6-dichlorohydroquinone, 2,6-bromohydroquinone, and 2,6-dimethylhydroquinone. To ensure that the absorbance change of the reaction mixture was within a measurable range, either a 1.0 cm path length cuvette with a 1.0 mL reaction volume or a 5.0 cm path length cuvette with a 2.0 mL reaction volume was used. The 1.0 cm path length cuvette was used for initial screening of possible substrates, for all of the inhibitor studies, for the substrate dependence steady-state kinetics of 2,6-dimethylhydroquinone, and for the O_2 dependence steady-state kinetics. In these studies, 5−10 μL of 85−110 μM PcpA was used. The 5.0 cm path length cuvette was used for the substrate dependence steady-state kinetic studies of 2,6-dichlorohydroquinone, 2,6-dibromohydroquinone, and 2-chloro-6-methylhydroquinone, in which 2.5 μL of 110 μM PcpA was used. For the initial screening of substrates, both high (200−400 μM) and low (10−60 μM) concentrations of the compounds in question were tested. Air-saturated 20 mM potassium phosphate buffer (pH 7.0) was used throughout. All reactions were performed at 23 °C. Because of the use of $NaBH_4$ for in situ reduction of the substituted benzoquinones to the corresponding hydroquinones, bubbles of H_2(g) formed during the course of the reaction, thereby causing a small baseline shift in the absorbance spectrum. To account for this absorbance shift, the baseline absorbance, measured at 380 nm, was subtracted from the product absorbance at each time point.

dx.doi.org/10.1021/bi200855m | *Biochemistry* 2011, 50, 8899−8913

For the initial screening of possible substrates, the spectrophotometric assay was conducted with a range of compounds, and changes in the UV−visible absorbance spectrum were monitored. For each compound tested, a control experiment in the absence of PcpA was conducted to ensure that enzymatic activity was the source of any spectral changes. The appearance of a new transition in the PcpA-containing reaction but not in the control was determined to be representative of ring-cleavage activity. Molecules that were determined to be cleaved by PcpA were further characterized by steady-state kinetics. The initial velocities were measured, divided by the enzyme concentration used, and plotted versus substrate concentration, and the Michaelis−Menten equation was fit to the data with KaleidaGraph (Synergy) to yield the K_{mA}^{app} and k_{cat}^{app} values in air-saturated buffer (O_2 concentration of 267−275 μM). The dependence of the O_2 concentration on the rate in the presence of high concentrations (200 or 300 μM) of the substrates was determined by the same spectrophotometric method, and the Michaelis−Menten equation was fit to the data to yield the apparent K_{mO_2} and k_{cat} values. The O_2 concentrations in the buffers were determined with an O_2-sensitive electrode (Hansatech) in separate control experiments without PcpA.

For the initial screening of inhibitors, the spectrophotometric assay was conducted with the compound in question at 500 μM and the native substrate at 50 μM, and the initial velocity relative to that without inhibitor was calculated. Detailed steady-state kinetic characterization was performed on three of the strongest inhibitors. Likewise, the kinetics of the monosubstituted hydroquinones were analyzed by treating them as inhibitors of 2,6-dichlorohydroquinone. For each inhibitor, the initial velocities were determined with five or six different substrate concentrations at each of three or four different inhibitor concentrations (and in the absence of inhibitor). The inhibition constant, K_I, was determined by performing a global fit to the data set using the Solver function of Excel (Microsoft). Only the value of K_I was allowed to float. The inhibitor studies were performed in the 1.0 cm path length cuvette, which was more convenient to use and required less material, whereas determination of the kinetic parameters of 2,6-dichlorohydroquinone required use of the 5.0 cm path length cuvette because of the low molar absorptivity of the product and the low K_{mA}^{app} for this compound. Use of only 1.0 cm path length data consistently led to a large overestimate of K_{mA}^{app}. Thus, in the fitting of the inhibitor data, the value of K_{mA}^{app} determined from the 5.0 cm path length data was kept fixed. The uncertainty in K_I was estimated by a jackknife procedure[53] and propagated with the uncertainty in K_{mA}^{app} by standard methods.

Enzyme inactivation with different compounds was assessed by several methods. (1) The curvature during product formation was directly observed in the spectrophotometric assay. Conditions under which the enzyme was completely inactivated before the substrate was consumed were used (0.46 μM enzyme and 50 μM substrate for the monosubstituted hydroquinones and 0.146 μM enzyme and 200−300 μM substrate for the *ortho*-disubstituted hydroquinones), and this was used to estimate the partition ratio:[38]

$$\text{partition ratio} = \frac{\text{moles of substrate consumed}}{\text{moles of enzyme inactivated}} = \frac{k_{cat}^{app}}{j_{inact}^{app}} \quad (1)$$

(2) PcpA was incubated both with and without the compound in question in either air-saturated buffer or O_2-free buffer, followed by addition of substrate (and more air-saturated buffer, in the latter case). (3) The curvature in the product formation of the native substrate when the compound in question was used as an inhibitor was fit to the equation

$$P_t = P_\infty(1 - e^{-j_s t}) + P_i \quad (2)$$

to yield the rate of inactivation, j_s (P_t, P_i, and P_∞ are the amounts of product formed at time t, at the start of the assay, and at time ∞, respectively). The apparent rate constant of inactivation, j_{inact}^{app}, and the apparent binding constant of inactivation, K_{inact}^{app}, were obtained by performing a global fit of the values of j_s as a function of the inactivating compound concentration, [I], at different substrate concentrations, [A], with Solver:

$$j_s = \frac{j_{inact}^{app}[I]}{K_{inact}^{app}(1 + [A]/K_{mA}^{app}) + [I]} \quad (3)$$

This procedure has been reported previously be Eltis and co-workers.[38]

Product Determination. PcpA reaction products were identified in two different ways. First, the aqueous reaction mixture (in an 86% H_2O/10% D_2O/4% CD_3OD mixture) was directly characterized by ^1H NMR spectroscopy, with sodium 3-(trimethylsilyl)-1-propanesulfonate (DSS) used as the chemical shift standard. For these reactions, PcpA was buffer exchanged into 20 mM potassium phosphate buffer (pH 7.0) and reconstituted with iron(II) anaerobically (without the use of imidazole) in a glovebox. The substrate concentration was 2.0 mM. Second, the aqueous reaction mixture was acidified to pH <2 with 1.0 M HCl, extracted with $CDCl_3$, dried over anhydrous Na_2SO_4, and characterized by ^1H NMR spectroscopy. To ensure that degradation of the ring-cleavage products did not occur, the ^1H NMR spectra of the aqueous reaction mixtures were recorded immediately after complete enzymatic cleavage had occurred as determined by UV−visible spectroscopy. Likewise, acidification and extraction into $CDCl_3$ were conducted the same day, and the ^1H NMR spectra were again recorded immediately. ^1H NMR spectroscopy was performed on a 400 MHz Bruker Avance III instrument.

RESULTS

Identification of Substrates. Four classes of compounds were tested as possible substrates of PcpA. The first class consisted of compounds with substituents at the 2, 4, and 6 positions of the ring like the physiological substrate but varying in the identity of those substituents: 2,6-dibromohydroquinone (2,6-diBrHQ), 2,6-dimethylhydroquinone (2,6-diMeHQ), 2-chloro-6-methylhydroquinone (2-Cl-6-MeHQ), 4-amino-2,6-dichlorophenol, and 3,5-dichloro-4-hydroxybenzoate. The second class consisted of monosubstituted hydroquinones (HQs): chloro-, bromo-, methyl-, and hydroxyhydroquinone (ClHQ, BrHQ, MeHQ, and HOHQ, respectively) and gentisate. The third class consists of *ortho*-disubstituted

Table 1. λ_{max} and Molar Absorptivity Values for the Reaction Products of Each of the Hydroquinone Substrates with PcpA in Air-Saturated 20 mM Potassium Phosphate Buffer (pH 7.0)[a]

substrate	reaction product	tautomer	λ_{max} (nm)	ε (M^{-1} cm^{-1})
2,6-dichlorohydroquinone (**1**)	2-chloromaleylacetate (**3**)	keto	253	9600[b]
2,6-dibromohydroquinone (**5**)	2-bromomaleylacetate (**7**)	keto	259	10600
2,6-dimethylhydroquinone (**9**)	2-methylmaleylacetone (**10**)	keto	254	7200
		enol	315	6300
2-chloro-6-methylhydroquinone (**12**)	mixture[c]	keto	250	8300
		enol	314	2500
chlorohydroquinone	maleylacetate	keto	248	~5100[d]
bromohydroquinone	maleylacetate	keto	248	~5100[d]
methylhydroquinone	maleylacetone	keto	240	nd[e]
		enol	310	

[a]For the *ortho*-disubstituted hydroquinones, the identities of the reaction products and their tautomeric states were determined by ^{1}H NMR studies. For the monosubstituted hydroquinones, the reaction products were tentatively assigned on the basis of the similarity of their UV−visible spectra with those reported previously for unsubstituted maleylacetate and maleylacetone. [b]In agreement with the value previously reported at pH 6.7 in potassium phosphate buffer.[30] [c]The reaction products consist of a mixture of 2-methylmaleylacetate (**14**), which exists entirely in the keto form, and 2-chloromaleylacetone (**16**), which exists as a mixture of keto and enol forms. The molar absorptivity reported here is for the product mixture obtained in air-saturated buffer. [d]Reported previously: 4000 M^{-1} cm^{-1} at 243 nm.[54] [e]Reported previously at pH 6.43: 4400 M^{-1} cm^{-1} at 243 nm and 9300 M^{-1} cm^{-1} at 312 nm.[55]

phenols and 3-substituted catechols: 2,6-dichlorophenol, 2,6-dibromophenol, 2,6-dimethylphenol, 2-chloro-6-methylphenol, 2-bromo-6-methylphenol, 3-methylcatechol, 3-bromocatechol, and pyrogallol. Lastly, catechol, 4-methylcatechol, 2,5-dichlorohydroquinone, and unsubstituted hydroquinone were also tested. Of these compounds, PcpA oxidatively cleaved 2,6-diBrHQ, 2,6-diMeHQ, and 2-Cl-6-MeHQ (as well as 2,6-diClHQ), and complete conversion to products (as shown by complete loss of the substrate features by UV−visible and ^{1}H NMR spectroscopy) could be obtained at all substrate concentrations. The λ_{max} and molar absorptivity values for these reaction products are summarized in Table 1.

PcpA also oxidatively cleaved ClHQ, BrHQ, and MeHQ. However, complete conversion to products was not observed even at low substrate concentrations (10−60 μM), except in some cases with very large amounts of PcpA. An example with BrHQ is shown in Figure 1. A difference spectrum shows that λ_{max} for this cleavage product is 248 nm. Accounting for the absorbance at 248 nm in the control reaction without PcpA, and estimating a molar absorptivity of the product when complete conversion was obtained with larger amounts of PcpA of ~5100 M^{-1} cm^{-1}, we found that only ~40% of the BrHQ in the reaction shown in Figure 1 was converted to product. As seen clearly in the plot of absorbance versus time (inset), most of the product formation occurred during the mixing time of the reaction, and the rate of reaction fell to zero well before the substrate was depleted. Similar results were obtained with ClHQ. With MeHQ, the difference spectrum showed transitions at 240 and 310 nm in an approximately 3:4 ratio, but complete conversion to products was never obtained. This behavior indicates that PcpA was rapidly inactivated by these substrates. Inactivation is a well-known phenomenon in EDOs with certain substrates such as 3-chlorocatechol in which a distinct curvature in the time course of product formation is observed.[36−39] Inactivation has been thoroughly characterized in *Burkholderia xenovorans* LB400 2,3-dihydroxybiphenyl 1,2-dioxygenase (BphC), where it has been shown to be due to loss of O_2 from the active site as superoxide, leaving the iron center in the inactive Fe(III) state.[38]

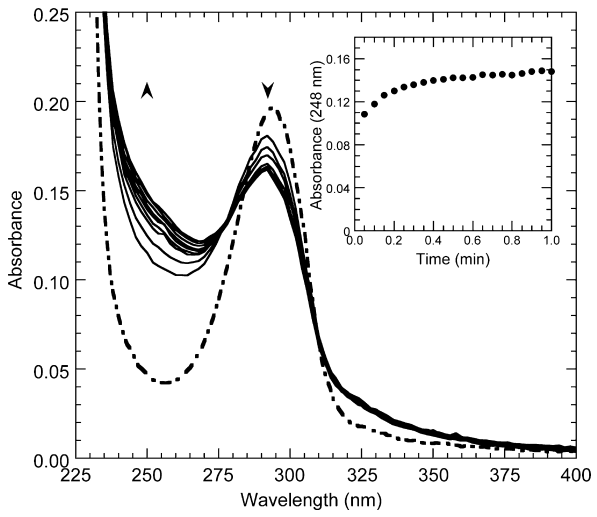

Figure 1. Absorbance spectrum of the ring cleavage of 50 μM BrHQ by 0.46 μM PcpA. The dashed line shows data for a control reaction without enzyme. The inset shows the time course for the absorbance change at 248 nm.

These results show that PcpA is a remarkably specific enzyme: only *ortho*-disubstituted HQs are good substrates. With monosubstituted HQs, ring cleavage is observed; however, these substrates rapidly inactivate PcpA, leading to only limited amounts of ring-cleavage product. PcpA did not detectably cleave substrates bearing an amino or carboxylate group at the 4 position. Other compounds that were not substrates for PcpA include 2,5-dichlorohydroquinone, unsubstituted hydroquinone, catechols, and gentisate. Therefore, PcpA requires hydroxyl groups at the 1 and 4 positions and substituents at the 2 and 6 positions of the aromatic ring for ring cleavage to occur without significant enzyme inactivation.

Characterization of the Ring-Cleavage Products. Xun and co-workers demonstrated by mass spectrometry that the ring-cleavage product of 2,6-diClHQ by PcpA was 2-chloromaleylacetate, which is the result of a 1,2-oxidative ring-cleavage reaction, followed by a rapid nonenzymatic hydrolysis of the acid chloride (species **2** in Scheme 2). We have characterized the ring-cleavage products of all four *ortho*-disubstituted HQs by ^{1}H NMR. The substrate 2-Cl-6-MeHQ is

Scheme 2. Ring-Cleavage Products of PcpA Substrates, Showing the Various Isomers Possible under Different Conditions

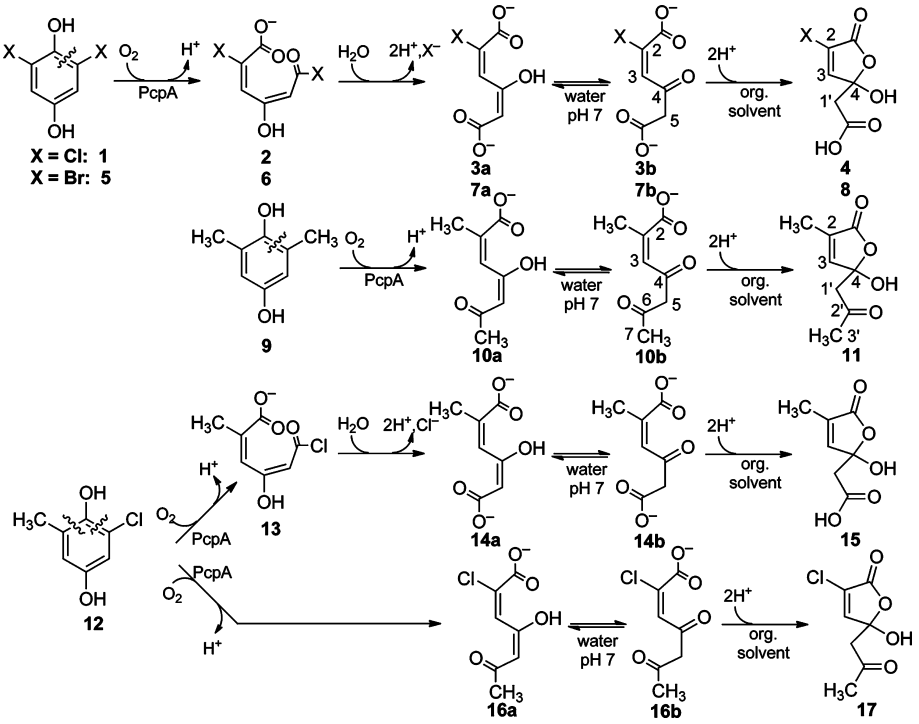

Table 2. ^{1}H NMR Spectra (400 MHz) of the Ring-Cleavage Products of the Four *Ortho*-Disubstituted Hydroquinone Substrates in an 86% H_2O/10% D_2O/4% CD_3OD Mixture at pH 7[a]

substrate	product	2-Me	3-H	5-H	7-H
2,6-dichlorohydroquinone (**1**)	**3b** (80%)		6.56 (s)	3.48 (s)	
	3b (20%)[b]		6.56 (s)	3.75 (s)	
2,6-dibromohydroquinone (**5**)	**7b** (79%)		6.74 (s)	3.46 (s)	
	7b (21%)[b]		6.73 (s)	3.73 (s)	
2,6-dimethylhydroquinone (**9**)	**10a** (37%)	2.02 (d, J = 1.6)	5.63 (q, J = 1.6)	5.69 (s)	2.12 (s)
	10b (63%)	2.02 (d, J = 1.6)	6.00 (q, J = 1.6)	3.82 (s)	2.26 (s)
2-chloro-6-methylhydroquinone (**12**)	**14b** (74%)	2.01 (d, J = 1.6)	6.10 (q, J = 1.6)	3.39 (s)	
	14b (13%)[b]	2.03 (d, J = 1.6)	6.06 (q, J = 1.6)	3.67 (s)	
	16a (6.5%)		6.19 (s)[c]	5.70 (s)	2.16 (s)[c]
	16b (6.5%)		6.51 (s)[c]	3.89 (s)	2.27 (s)[c]

[a]The chemical shifts are reported vs TSP. Scalar couplings are reported in hertz. [b]Note that in all of the 2-substituted maleylacetates, a second form is present at ~20% that is also consistent with a keto tautomer. This may represent a second isomer of the same compound that is in slow exchange. For example, partial double-bond character in the C3−C4 bond of these conjugated systems could lead to the observation of separate signals for the *s-cis* and *s-trans* forms, although we cannot rule out other options. [c]Although the integration values do not differ, we have offered tentative assignments based on the similarities of the chemical shifts to those of the enol and keto forms of 2-methylmaleylacetone (**10a** and **10b**, respectively).

of particular interest, because cleavage between the hydroxyl group and the *ortho* substituents could result in two different products, and the ratio of these products could provide insight into the factors that determine substrate specificity.

These ring-cleavage products can exist as different isomers under different conditions (Scheme 2) as discussed previously in the literature for maleylacetates[56,57] and maleylacetones.[55,58−60] At approximately neutral pH in water, unsubstituted maleylacetate exists entirely in the keto form[57] and unsubstituted maleylacetone exists as a mixture of the keto and enol forms.[55,58] Under acidic conditions (and subsequent extraction into organic solvents), these compounds cyclize to form lactones. To determine both the regiospecificity of ring cleavage and to identify the isomeric forms, we characterized these ring-cleavage products by ^{1}H NMR under conditions that corresponded to those of the kinetic experiments and previous literature reports: in an 86% H_2O/10% D_2O/4% CD_3OD mixture at pH 7 (Table 2) and after acidification to pH <2 and extraction into $CDCl_3$ (Table S1 of the Supporting Information).

The ^{1}H NMR spectra of the ring-cleavage products in water at pH 7 show that the oxidative ring cleavage of 2,6-diClHQ and 2,6-diBrHQ yields 2-chloromaleylacetate and 2-bromomaleylacetate, respectively, and that these species exist exclusively as the keto form [(*E*)-2-chloro-4-oxohex-2-enedioate (**3b**) and (*E*)-2-bromo-4-oxohex-2-enedioate (**7b**), respectively]. The ring-cleavage product of 2,6-diMeHQ exists as a mixture of 37% of the enol form and 63% of the keto form of 2-methylmaleylacetone [(2*Z*,4*E*)-4-hydroxy-2-methyl-6-oxohepta-2,4-dienoate (**10a**) and (*Z*)-2-methyl-4,6-dioxohept-2-enoate (**10b**),

dx.doi.org/10.1021/bi200855m | *Biochemistry* 2011, 50, 8899−8913

respectively]. In both forms, the C2 methyl group and the 3-H proton are *cis* to each other on the basis of the coupling constant. However, we cannot determine the orientation of the C4=C5 bond of the enol form. The ^{1}H NMR spectrum of the ring-cleavage product of 2-Cl-6-MeHQ shows a mixture of four species. Two species are the two different keto isomers of 2-methylmaleylacetate (similar to what was observed with the 2-halomaleylacetates), resulting from cleavage of the substrate between the hydroxyl and chloro substituents (1,2-cleavage). The other two species are the keto and enol forms of 2-chloromaleylacetone, resulting from cleavage of the substrate between the hydroxyl and methyl group (1,6-cleavage). Overall, the integrations of the signals yield 74 and 13% of the two keto isomers of 2-methylmaleylacetate [(*Z*)-2-methyl-4-oxohex-2-enedioate (**14b**)] and 6.5% each for the enol and keto forms of 2-chloromaleylacetone [(2*E*,4*E*)-2-chloro-4-hydroxy-6-oxohepta-2,4-dienoate (**16a**) and (*E*)-2-chloro-4,6-dioxohept-2-enoate (**16b**), respectively]. Thus, the reaction of 2-Cl-6-MeHQ with PcpA yields 87% 1,2-cleavage and 13% 1,6-cleavage.

The UV−visible absorption spectra of the cleavage products can be interpreted in the context of the NMR data in pH 7 water. The cleavage products of 2,6-diClHQ and 2,6-diBrHQ show a single transition at 253 and 259 nm, respectively, and the NMR spectra show that these species exist exclusively as the keto tautomer. The 2,6-diMeHQ cleavage product shows two transitions at 250 and 314 nm, and the NMR spectrum shows that it exists as a mixture of the keto (63%) and enol (37%) forms. Thus, the transition at 250−260 nm corresponds to the keto form, and the transition at 314 nm corresponds to the enol form, as expected from empirical rules for the UV−visible absorption spectra of organic molecules.[61] The UV−visible absorption spectrum of the cleavage products of 2-Cl-6-MeHQ shows transitions at 250 and 314 nm, with the latter much less intense than the former. The NMR spectrum showed that it is a mixture of 87% keto form 2-methylmaleylacetate (**14b**) and 13% 2-chloromaleylacetone in a ∼1:1 keto:enol ratio (**16a** and **16b**). However, the conditions used for NMR differed from those used for the kinetic experiments (higher substrate concentration and much longer reaction time), and consequently, the 314 nm to 250 nm ratio was lower (for reasons explained in the subsequent section on kinetics). When we account for this, the ratio of products observed under the conditions used for kinetics in air-saturated buffer can be estimated to be 68% 2-methylmaleylacetate and 32% chloromaleylacetone. Pure 2-methylmaleylacetate in water has been reported to have a single transition at 250 nm with a molar absorptivity of 9600 M^{-1} cm^{-1}.[54] From this, we can estimate the molar absorptivity of chloromaleylacetone to be 7800 and 5500 M^{-1} cm^{-1} at 314 and 250 nm, respectively. This is in reasonable agreement with our results for methylmaleylactone, considering the higher enol:keto ratio.

Because only very limited amounts of the cleavage products of the monosubstituted HQs could be produced, they were characterized by only UV−visible absorption spectroscopy. The cleavage products of ClHQ and BrHQ yielded identical absorption spectra with a λ_{max} at 248 nm and a molar absorptivity of ∼5100 M^{-1} cm^{-1}, in reasonable agreement with what has been reported for unsubstituted maleylactate.[54] The two transitions at 240 and 310 nm in the cleavage product of MeHQ are consistent with what has been reported for unsubstituted maleylacetone: 4400 M^{-1} cm^{-1} at 243 nm and 9300 M^{-1} cm^{-1} at 312 nm.[55] Thus, these data are consistent with at least predominant 1,2-cleavage of the monosubstituted HQs.

Kinetic Parameters of Hydroquinone Substrates. Results of steady-state kinetic studies of the four *ortho*-disubstituted HQs in air-saturated buffer (267−275 μM O_2) are shown in Figure 2. The steady-state kinetic parameters are listed in Table 3.

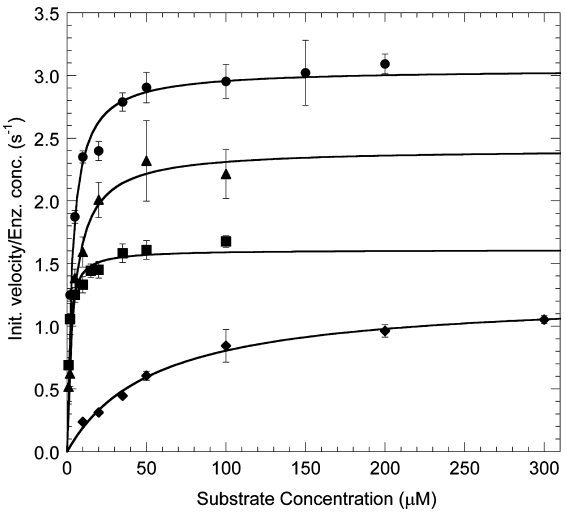

Figure 2. Steady-state kinetics of PcpA with *ortho*-disubstituted hydroquinones: (●) 2,6-diClHQ, (■) 2,6-diBrHQ, (◆) 2,6-diMeHQ, and (▲) 2-Cl-6-MeHQ. The dependence of the hydroquinone substrate concentration on the initial velocity was determined in air-saturated (267−275 μM O_2) buffer, and the curves are fits of the Michaelis−Menten equation to the data.

PcpA exhibited the following trend in apparent specificity constant ($k_{cat}^{app}/K_{mA}^{app}$) among the *ortho*-disubstituted HQs: 2,6-diBrHQ ∼ 2,6-diClHQ > 2-Cl-6-MeHQ ≫ 2,6-diMeHQ. While PcpA had a similar apparent specificity for 2,6-diClHQ and 2,6-diBrHQ, both the K_{mA}^{app} and k_{cat}^{app} values for the latter were lower. 2,6-diMeHQ was turned over more slowly than the dihalo-HQs and also had a significantly higher Michaelis constant. Thus, relative to that of 2,6-diClHQ, the $k_{cat}^{app}/K_{mA}^{app}$ was reduced ∼40-fold. As described above, 2-Cl-6-MeHQ yields a mixture of cleavage products: the transition at 250 nm comes from the keto forms of both 2-methylmaleylacetate (the major product, **14b**) and 2-chloromaleylacetone (**16b**), while the transition at 314 nm is from the enol form of 2-chloromaleylacetone (**16a**). Analysis of the rate data at the two wavelengths yielded K_{mA}^{app} values within the error bars. Moreover, the ratio of products was invariant with substrate concentration. Thus, k_{cat}^{app} was evaluated by treating the mixture as a single product with the effective molar absorptivity reported in Table 1. Relative to those of 2,6-diClHQ, the apparent specificity constant of 2-Cl-6-MeHQ was approximately half, k_{cat}^{app} was somewhat lower, and K_{mA}^{app} was only slightly greater. Thus, the behavior of 2-Cl-6-MeHQ in air-saturated buffer much more closely matches that of the dihalo-HQs than it does that of 2,6-diMeHQ.

Partition ratios were estimated at high substrate concentrations (300 μM for 2,6-diMeHQ and 200 μM for the other *ortho*-disubstituted HQs) and low enzyme concentrations, such that the enzyme was completely inactivated before all of the substrate was consumed (Table 3). Unlike with the

Table 3. PcpA Steady-State Kinetic Parameters Measured with Hydroquinone Substrates in Air-Saturated Buffer

substrate	K_{mA}^{app} (μM)	k_{cat}^{app} (s^{-1})	$k_{cat}^{app}/K_{mA}^{app}$ (s^{-1} μM^{-1})	partition ratio	j_{inact}^{app} (s^{-1})
2,6-dichlorohydroquinone (**1**)	3.2 ± 0.3	3.05 ± 0.05	1.0 ± 0.1	~700	~0.004[a]
2,6-dibromohydroquinone (**5**)	1.3 ± 0.2	1.61 ± 0.03	1.2 ± 0.1	~400	~0.004[a]
2,6-dimethylhydroquinone (**9**)	55 ± 6	1.25 ± 0.05	0.023 ± 0.003	~500	~0.003[a]
2-chloro-6-methylhydroquinone (**12**)	4.4 ± 0.7	2.41 ± 0.09[b]	0.54 ± 0.08	~800	~0.003[a]
chlorohydroquinone	10 ± 1[c]	~2[d]	~0.2	~40	0.046 ± 0.008
bromohydroquinone	8.5 ± 1.0[c]	~1[d]	~0.1	~40	0.027 ± 0.003
methylhydroquinone	41 ± 5[c]	nd[e]	nd[e]	~8	nd[e]

[a]Estimated from the partition ratio and k_{cat}^{app} (eq 1). [b]Treating the product mixture as a single species with an effective molar absorptivity at 250 nm of 8300 M^{-1} cm^{-1}. [c]K_{mA}^{app} was determined by measuring the competitive inhibition of 2,6-diClHQ by these substrates (K_I). For ClHQ and BrHQ, it was also determined by fits to the curvature in the time course of product formation (K_{inact}^{app}). The value was the same within the error bars for ClHQ and somewhat lower (4.6 ± 1.1 μM) for BrHQ. [d]Estimated from the partition ratio and j_{inact}^{app} (eq 1). [e]Not determined.

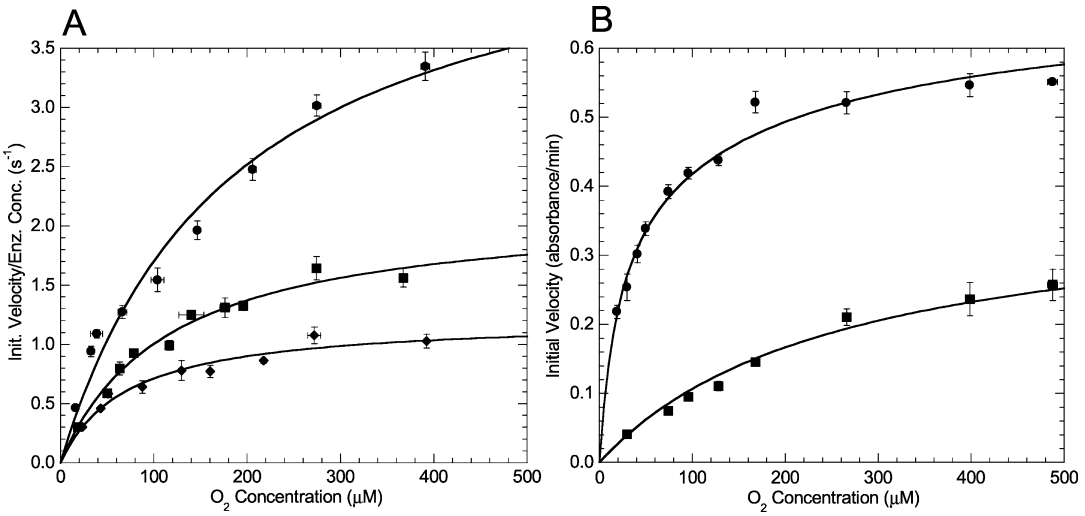

Figure 3. Steady-state kinetics of PcpA with *ortho*-disubstituted hydroquinones. (A) Dependence of the O_2 concentration on the initial velocity at high substrate concentrations (300 μM for 2,6-diMeHQ and 200 μM for the others): (●) 2,6-diClHQ, (■) 2,6-diBrHQ, and (◆) 2,6-diMeHQ. The curves are fits of the Michaelis–Menten equation to the data. (B) O_2 dependence of the steady-state cleavage of 2-Cl-6-MeHQ (200 μM) by PcpA as monitored at 250 (●) and 314 nm (■). The curves are simultaneous fits of both data sets accounting for different kinetic parameters for the two cleavage modes and for the molar absorptivities of the two products.

Table 4. Steady-State Kinetic Parameters for the O_2 Dependence of PcpA for the *Ortho*-Disubstituted Hydroquinones

substrate	K_{mO_2} (μM)[a]	k_{cat} (s^{-1})[a]	k_{cat}/K_{mO_2} (s^{-1} μM^{-1})
2,6-dichlorohydroquinone (**1**)	190 ± 40	4.8 ± 0.5	0.026 ± 0.006
2,6-dibromohydroquinone (**5**)	120 ± 20	2.2 ± 0.1	0.019 ± 0.003
2,6-dimethylhydroquinone (**9**)	70 ± 10	1.4 ± 0.2	0.020 ± 0.005
2-chloro-6-methylhydroquinone (**12**) 1,2-cleavage	21 ± 3	1.58 ± 0.06	0.07 ± 0.01
2-chloro-6-methylhydroquinone (**12**), 1,6-cleavage	260 ± 60	1.8 ± 0.2	0.007 ± 0.002

[a]Because these data were obtained at a saturating concentration of the organic substrate (>40-fold above K_{mA}^{app}) for 2,6-diClHQ and 2,6-diBrHQ, the direct fit of the O_2 dependence data with the Michaelis–Menten equation yields the true value of k_{cat}, and the $K_{mO_2}^{app}$ should be approximately equal to the true K_{mO_2} (a 10-fold difference between K_{dA} and K_{mA} would give a difference between $K_{mO_2}^{app}$ and K_{mO_2} of <15%). For 2,6-diMeHQ, the k_{cat}^{app} obtained from the O_2 dependence data was corrected for the nonsaturating substrate concentration, and $K_{mO_2}^{app}$ and K_{mO_2} may differ by more than those for the other substrates. For 2-Cl-6-MeHQ, these values are $K_{mO_2}^{app}$ and k_{cat}^{app}, rather than K_{mO_2} and k_{cat}.

monosubstituted HQs, complete inactivation of PcpA by the disubstituted HQs occurred slowly (~10 min for the dihalo-HQs and >1 h for 2-Cl-6-MeHQ and 2,6-diMeHQ). Given the length of time required for inactivation, these values should be viewed with some caution and may be lower limits on the actual partition ratios. In particular, the dihalo-HQs air-oxidize to the corresponding benzoquinones on this time scale, and the presence of minute quantities of the benzoquinone was itself found to reduce the rate of ring cleavage. The partition ratios for the disubstituted HQs were all fairly similar. From the partition ratios and the k_{cat}^{app} values, the rates of enzyme inactivation (j_{inact}^{app}) with these substrates were estimated. These values were very similar for the four disubstituted HQs.

Because the monosubstituted HQs rapidly inactivate PcpA, initial rate data could not be obtained easily. Therefore, 2,6-diClHQ was used as a reporter substrate, treating the monosubstituted HQs as competitive inhibitors. The resulting K_I from fits to these inhibition data yielded the K_{mA}^{app} for these substrates (Table 3). Also, the curvature in the time course of product formation was fit, and the resulting exponential terms (j_s)

dx.doi.org/10.1021/bi200855m | *Biochemistry* 2011, 50, 8899–8913

were plotted as a function of monosubstituted HQ concentration at different 2,6-diClHQ concentrations and fit with a competitive inhibition-type equation (eq 3), in which 2,6-diClHQ inhibits the enzyme inactivation caused by one of these compounds. The resulting apparent rate constants of inactivation, j_{inact}^{app}, are listed in Table 3. Qualitatively, MeHQ showed less curvature, thus precluding an accurate fit to the j_s data. Partition constants were estimated, and from the partition constants and j_{inact}^{app} values, k_{cat}^{app} and in turn $k_{cat}^{app}/K_{mA}^{app}$ were estimated for ClHQ and BrHQ. The k_{cat}^{app} values were only somewhat lower than those for the dihalo-HQs, and the specificity constants were between those of the dihalo-HQs and 2,6-diMeQ. The most notable difference between the dihalo-HQs and ClHQ and BrHQ is that for the latter substrates the partition ratio was ~10-fold lower and, correspondingly, j_{inact}^{app} was ~10-fold higher.

Thus, overall, it appears that there is an interaction between the *ortho* substituents of the substrate and the active site that significantly affects $k_{cat}^{app}/K_{mA}^{app}$ and modestly affects k_{cat}^{app}, indicating that this interaction leads to a much greater specificity for HQs with halogen substituents versus methyl substituents. Furthermore, the removal of one *ortho* substituent greatly increases the rate of inactivation.

Kinetic Parameters of O_2. The O_2 dependence on the initial velocities for 2,6-diClHQ, 2,6-diBrHQ, and 2,6-diMeHQ at high substrate concentrations is shown in Figure 3A, and the resulting kinetic parameters are listed in Table 4. The k_{cat}/K_{mO_2} values were remarkably similar for these three symmetric substrates, and both the K_{mO_2} and k_{cat} values for these substrates shared the same trend: 2,6-diClHQ > 2,6-diBrHQ > 2,6-diMeHQ.

In the presence of saturating amounts of 2-Cl-6-MeHQ, the ratio of cleavage products was strongly dependent on O_2 concentration. Thus, the initial rates of the increase in absorbance at 250 and 314 nm displayed different dependencies on O_2 concentration (Figure 3B). Several mechanisms were considered in which a single organic substrate could bind to the enzyme to yield two different products. A mechanism consistent with the observation that the product ratio is invariant with respect to substrate concentration but varies with O_2 concentration is shown in Scheme 3. This yields the following equations for the initial rates of formation for the two products

$$V = \frac{dP}{dt} = (N_1[A][O_2][E_t] + N_2[A][O_2]^2[E_t]) / (D_1 + D_2[O_2] + D_3[A] + D_4[O_2]^2 + D_5[A][O_2] + D_6[A][O_2]^2) \quad (4)$$

$$V' = \frac{dQ}{dt} = (N_3[A][O_2][E_t] + N_4[A][O_2]^2[E_t]) / (D_1 + D_2[O_2] + D_3[A] + D_4[O_2]^2 + D_5[A][O_2] + D_6[A][O_2]^2) \quad (5)$$

where [A], [O_2], and [E_t] are the concentrations of the HQ substrate, O_2, and enzyme, respectively, and the N_x and D_x coefficients are functions of the rate constants from the mechanism in Scheme 3 (see the Supporting Information for the derivations and for the definition of these coefficients). At a fixed [O_2], because the denominator terms of V and V' are identical and the numerator is first-order in [A], then the ratio of product formation as function of [A] is constant (in agreement with experiment) and the initial rates should follow Michaelis–Menten kinetics with the following equations for k_{cat}^{app} and K_{mA}^{app}:

Scheme 3. Mechanism by Which 2-Cl-6-MeHQ Binds to PcpA in Two Different Orientations Yielding Two Different Products

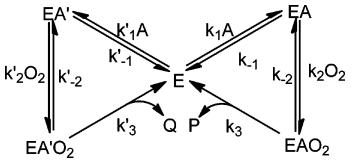

$$k_{cat}^{app} = \frac{N_1[O_2] + N_2[O_2]^2}{D_3 + D_5[O_2] + D_6[O_2]^2} \quad (6)$$

$$k'^{app}_{cat} = \frac{N_3[O_2] + N_4[O_2]^2}{D_3 + D_5[O_2] + D_6[O_2]^2} \quad (7)$$

$$K_{mA}^{app} = \frac{D_1 + D_2[O_2] + D_4[O_2]^2}{D_3 + D_5[O_2] + D_6[O_2]^2} \quad (8)$$

At a fixed [A], the initial rates do not follow true Michaelis–Menten kinetics. However, if the terms in eqs 4 and 5 that are second-order in [O_2] are small, the O_2 dependence will still show saturation behavior that can be fit to a Michaelis–Menten type of equation; however, the resulting k_{cat}^{app} and $K_{mO_2}^{app}$ values cannot be related back to the N_x and D_x terms. The ratio of the initial rates of formation of the two products as a function of [O_2] is

$$\frac{V}{V'} = \frac{N_1 + N_2[O_2]}{N_3 + N_4[O_2]} \quad (9)$$

consistent with the experimentally observed nonlinear O_2 dependence on this ratio. Importantly, a mechanism in which the asymmetric substrate is in rapid equilibrium between the two binding modes without dissociating from the enzyme does not yield the observed dependence of the O_2 concentration on the product ratio, nor does a mechanism in which the substrate binds in a single orientation and then partitions between two different ring-cleavage pathways. However, there may be other mechanistic possibilities consistent with this observation, such as one binding mode leading to partial enzyme inactivation. This behavior in which a single substrate yields two different products with the same K_{mA}^{app} values but different $K_{mO_2}^{app}$ values has been observed before in a ring-cleaving dioxygenase. It was first reported in *Pseudomonas arvilla* catechol 1,2-dioxygenase (an IDO) with the substrate 3-methylcatechol, which led to a mixture of 1,2- and 2,3-cleavage products, although a detailed analysis of the kinetics was not performed.[62]

The transition at 314 nm arises from just the 1,6-cleavage product, while the transition at 250 nm arises from both products. Therefore, the initial rates of increase at both wavelengths were simultaneously fit with two Michaelis–Menten

equations (Figure 3, solid lines) with different k_{cat}^{app} and $K_{mO_2}^{app}$ values and with the reported molar absorptivity at 250 nm of the 1,2-cleavage product (2-methylmaleylacetate)[54] and the estimated molar absorptivities of the 1,6-cleavage product (chloromaleylacetone) at both 250 and 314 nm calculated above. This yielded the k_{cat}^{app} and $K_{mO_2}^{app}$ values for 1,2- and 1,6-cleavage listed in Table 3. Notably, the k_{cat}^{app} values are similar, while the $K_{mO_2}^{app}$ values differ ~10-fold. Although there is considerable uncertainty in the molar absorptivity of chloromaleylacetone at 250 nm, even a 50% error in this value changes the $K_{mO_2}^{app}$ values by <40% and preserves the ~10-fold difference in $K_{mO_2}^{app}$ between the two binding modes. These $K_{mO_2}^{app}$ values cannot be directly compared to those obtained for the symmetric substrates, because the value for the asymmetric substrate has a complex dependence on the rate constants of both pathways resulting from the two different binding modes. Nonetheless, it appears that the substituent external to the site of ring cleavage affects the O_2 dependence of the kinetics. The product resulting from cleavage between the chloro and hydroxyl groups has the lower $K_{mO_2}^{app}$ (the methyl group is external), and likewise, among the symmetric substrates, 2,6-diMeHQ has the lowest $K_{mO_2}^{app}$.

Identification and Kinetic Characterization of Inhibitors. The same molecules that were screened as possible substrates for PcpA were also tested as inhibitors. For those that were found to inhibit PcpA, the initial rate with 50 μM 2,6-diClHQ and 500 μM inhibitor is reported as a percentage relative to the rate without inhibitor in Table 5. The uncertainty was estimated to be approximately ±4%. Under these conditions, gentisate, catechol, 3-methylcatechol, 4-methylcatechol, and unsubstituted hydroquinone showed no evidence of inhibiting PcpA. Even 5.0 mM unsubstituted hydroquinone did not significantly inhibit 2,6-diClHQ cleavage (i.e., <3%). Thus, although removing just one of the four substituents on the ring results in a loss of PcpA's ability to cleave it (without significant inactivation), most of these compounds are still able to act as inhibitors.

Table 5. Inhibitors of PcpA

inhibitor	relative initial rate (±4%)[a]	K_I (μM)
2,6-dibromophenol	30%	13 ± 2
3-bromocatechol	57%	53 ± 7
		3800 ± 800[b]
2,6-dichlorophenol	66%	48 ± 6
4-amino-2,6-dichlorophenol	67%	nd[c]
pyrogallol	70%	nd[c]
2-bromo-6-methylphenol	83%	nd[c]
2,6-dimethylphenol	88%	nd[c]
2-chloro-6-methylphenol	90%	nd[c]

[a]With 50 μM 2,6-diClHQ and 500 μM inhibitor. [b]This compound is a mixed-mode inhibitor. The first number gives the K_I for the competitive inhibition component and the second that for the uncompetitive inhibition component. [c]Not determined.

The three strongest inhibitors (2,6-dibromophenol, 2,6-dichlorophenol, and 3-bromocatechol) were examined in more detail. 2,6-Dibromo- and 2,6-dichlorophenol were competitive inhibitors of PcpA versus 2,6-diClHQ, while 3-bromocatechol was a mixed-mode inhibitor. This confirms that these three compounds bind at the active site in a manner similar to that of the substrates and with a relatively high affinity, even though they cannot be cleaved. The trend in inhibitor strength as a function of *ortho* substituent mirrored the trend seen in the K_{mA}^{app} and $k_{cat}^{app}/K_{mA}^{app}$ values of the substrates. Bromo-substituted compounds were stronger inhibitors than the corresponding chloro-substituted compounds, which in turn were much stronger inhibitors than the methyl-substituted compounds. Hydroquinone, which lacks *ortho* substituents, did not inhibit to a detectable extent.

The capacity of the inhibitors 2,6-dichlorophenol, 2,6-dibromophenol, and 3-bromocatechol to inactivate PcpA was explored. PcpA was incubated for 15 s in air-saturated buffer either with or without one of the compounds in question, and then 2,6-diClHQ was added to a final concentration of 200 μM. The concentration of the potential inactivator was kept sufficiently low so that no diminution of the initial velocity could be observed due to competitive inhibition. The initial velocity was measured and compared to that obtained by the usual method, in which PcpA is added last to air-saturated buffer containing substrate and inhibitor. The monosubstituted HQs (known inactivators of PcpA) were tested as well for comparison. With 2,6-dibromophenol and 2,6-dichlorophenol, no significant difference was observed in the relative initial velocity (93−100%) compared to that for incubation with just air-saturated buffer (93 ± 6%). With the monosubstituted HQs and with 3-bromocatechol, a large amount of enzyme inactivation was observed after just 15 s [relative initial velocities of 26−47% (see Table S2 of the Supporting Information for details)]. Control experiments in which PcpA was incubated with these compounds under anaerobic conditions for several minutes prior to being mixed with air-saturated buffer and substrate showed no inactivation, indicating that the inactivation is O_2-dependent. This suggests that inactivation of PcpA, either by the monosubstituted HQs or by 3-bromocatechol, may arise from oxidation of the Fe(II) center.

The potential of the three strongest inhibitors to inactivate PcpA was also examined by measuring the curvature in the time course of product formation (with 2,6-diClHQ as the substrate) in the presence of each of the inhibitors, which was reported above for the monosubstituted HQs. With 2,6-dichloro- and 2,6-dibromophenol, the small increase in the curvature with an increasing amount of inhibitor could be entirely ascribed to substrate depletion, based on simulated data from the integrated rate equation[63] (see Figure S1 of the Supporting Information for a comparison of ClHQ with 2,6-dibromophenol). In contrast, 3-bromocatechol showed a much larger degree of curvature, which was also seen with the monosubstituted HQs. From fits to the curvature data, the K_{inact}^{app} and j_{inact}^{app} values of 3-bromocatechol were 40 ± 20 μM and 0.04 ± 0.01 s^{-1}, respectively. This is consistent with a model in which 3-bromocatechol competes with the substrate for the active site, and some fraction of inhibitor binding events leads to the irreversible inactivation of the enzyme.

DISCUSSION

Structural Requirements for Substrate and Inhibitor Binding. The structural requirements for substituted arenes to bind to the active site of PcpA are quite remarkable, and even more striking are the stringent requirements for aromatic ring cleavage (summarized in Figure 4). We will first address the role of the *para* and *ortho* substituents and then discuss the issue of catechol binding to PcpA.

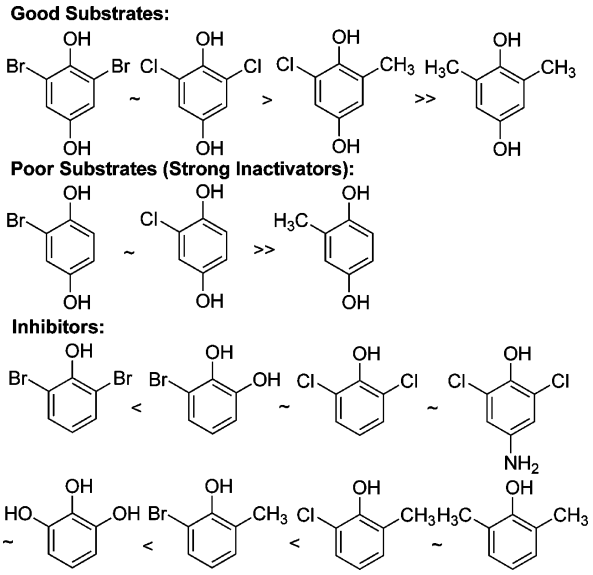

Figure 4. Structures of the substrates and inhibitors of PcpA, ranked in order of $k_{cat}^{app}/K_{mA}^{app}$ (for substrates) and K_I or inhibition strength at fixed concentrations (for inhibitors). Among the inhibitors, 2,6-dibromo- and 2,6-dichlorophenol do not inactivate the enzyme but 3-bromocatechol does, while the others have not been tested for inactivation.

The *p*-hydroxyl group plays a key mechanistic role, because it is an absolute requirement for ring cleavage. It also appears to contribute to the binding strength, which in turn suggests possible hydrogen bonding to this substituent from the protein. Hydrogen bonding to the substrate *p*-hydroxyl group has been implicated in gentisate[20] and homogentisate dioxygenases.[64] However, a *p*-amino group does not have the same effect on binding, as shown by the comparable amounts of inhibition between 4-amino-2,6-dichlorophenol and 2,6-dichlorophenol, which was also observed with the inhibition of gentisate dioxygenase.[16]

The *ortho* substituents play a key role in the binding of both substrates and inhibitors. Notably, unsubstituted hydroquinone did not inhibit the enzyme to a measurable extent up to a concentration of 5 mM (100-fold higher than the substrate concentration). The $k_{cat}^{app}/K_{mA}^{app}$ values of 2,6-diClHQ and 2,6-diBrHQ are ~40-fold higher than that of 2,6-diMeHQ. Likewise, the 2,6-dihalophenols are significantly stronger inhibitors than 2,6-dimethylphenol. The importance of *ortho* substituents for binding and the apparent trend in binding (Br > Cl ≫ CH_3) among both substrates and inhibitors suggest a specific interaction between *ortho* halo substituents and the protein. Because methyl and chloro groups are similar in size, it is not likely that this preference is solely due to steric requirements. This trend could result from either halogen bonding[65−69] or metal−halogen secondary bonding.[70] In halogen bonding, the halogen in a C−X bond interacts with the partial negative charge on an oxygen or nitrogen atom[65,67,69] or with the π electrons from an aromatic ring.[66,68] Interestingly, the strength of the halogen bond increases with halogen polarizability, which follows the same trend observed in the binding of substrates and inhibitors in PcpA. In *o*-chlorophenolate transition metal complexes, metal−halogen secondary bonding has been observed at a metal−chlorine distance of up to ~1.0 Å beyond the normal metal−chloride bond distance.[71,72] In complexes of iron(II) coordinated to a facial-capping tridentate ligand and *o*-chloro- and bromophenolates designed as simple structural models of PcpA, we observed metal−halogen distances that met this criterion for secondary bonding.[73] The energetics of metal−halogen secondary bonding have not been explored. However, it is thought that the strength of this interaction also increases with the polarizability of the halogen.[70]

In the EDOs, catechols are known to bind as monoanions that coordinate the iron(II) as bidentate ligands. One might expect that catechol derives a significant amount of its free energy of binding from ligation of the *o*-hydroxyl group to the iron(II) center, and that this interaction would be stronger than the sort of noncanonical halogen interactions discussed above. Thus, a bidentate ligand such as a catechol would have a higher binding strength than monodentate ligands such as *o*-dihalophenols. However, the opposite trend is observed in PcpA: of the catechols tested, only 3-bromocatechol and pyrogallol showed any evidence of inhibition of PcpA. 2,6-Dibromophenol was a stronger inhibitor than 3-bromocatechol, and even 2,6-dimethylphenol was a weak inhibitor; 3-methylcatechol did not detectibly inhibit PcpA. In comparison, while 2-halophenols are inhibitors of the well-studied EDO *P. putida* mt-2 catechol 2,3-dioxygenase (XylE), the K_I values of these inhibitors are more than 10-fold higher than those of inhibitors expected to be bidentate ligands, such as 2-aminophenol and 2-hydroxypyridine *N*-oxide.[74−76] It could be that ligation of the *o*-hydroxyl group to the iron(II) center contributes less to the free energy of binding than specific noncovalent interactions between the rest of the substrate or inhibitor and the active site in a given enzyme (hydrogen bonding to the *o*-hydroxyl group in EDOs vs halogen bonding to the *ortho* substituents in the case of PcpA). Alternatively, the shape of the substrate binding pocket in PcpA may force the *ortho* substituents to be too distant from the iron(II) for an *o*-hydroxyl group to coordinate, leaving noncovalent interactions between the protein and the *ortho* substituents as the only option.

Insights into the Mechanism of Ring Cleavage in PcpA. A generally accepted mechanism exists for EDOs, based upon experiments[6,7,10−12] and DFT calculations.[13,14] Substrate binds to the Fe(II) as a monoanion, with the hydroxyl group at the 2 position deprotonated. Next, O_2 binds, which induces deprotonation of the remaining substrate hydroxyl proton. The ternary complex is best described as an Fe(II)−superoxide−semiquinone ternary complex. The superoxide attacks at the 2 position, resulting in an alkylperoxide intermediate. A Criegee rearrangement of this alkylperoxide—specifically, an alkenyl migration—leads to a lactone, which is finally cleaved by nucleophilic attack of the iron(II)-bound hydroxide. This rearrangement may occur in multiple steps via epoxide and/or gem-diol intermediates.[12,14] It is believed that the structure of the alkylperoxide intermediate and its rearrangement via an alkenyl migration are the key features that lead to extradiol catechol ring cleavage, whereas an acyl migration leads to intradiol catechol ring cleavage in the Fe(III)-dependent IDOs.[6]

To date, essentially nothing is known about the mechanism of ring cleavage in PcpA or any of the other HQDOs. Although there must be important differences between the mechanism of PcpA and that of the EDOs, given that both use an Fe(II) ligated by a common facial-capping triad ligand set, it is likely that there are also many similarities. Thus, the EDO mechanism can be used to inform discussion of a mechanism for PcpA. As a

Scheme 4. Plausible Mechanism of PcpA[a]

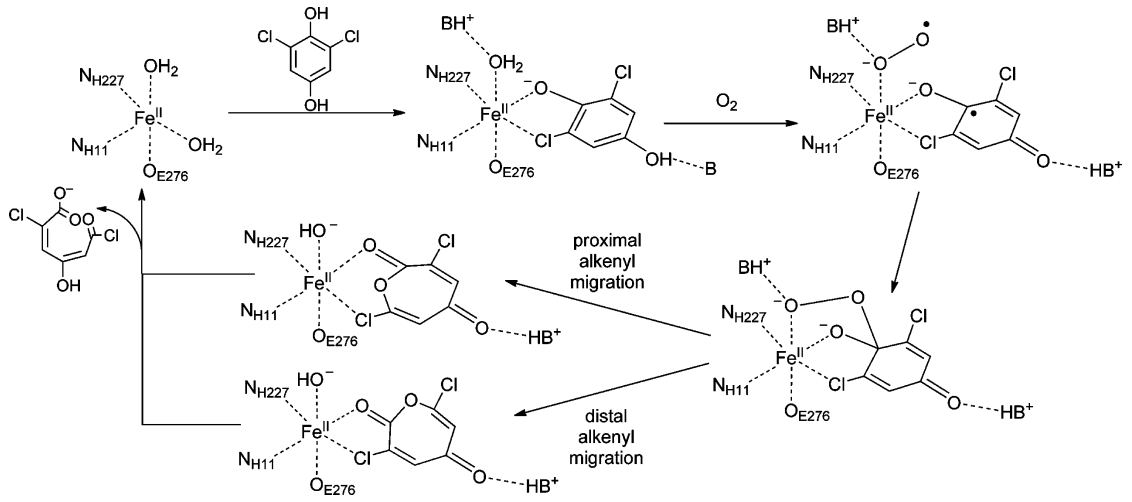

[a]Metal−ligand bonds are shown as dashed lines, and charges are shown explicitly. A dashed line is shown between one of the *o*-chloro substituents and the Fe(II), to suggest that one of the substituents could be close enough to form a metal−halogen secondary bond; however, the mechanism in no way requires this to be the case. Two possible alkenyl migrations are shown, distal and proximal. Only one of these is operative; however, the available data cannot be used to determine which is operative.

result of this work, there are three key observations that must be explained by any postulated mechanism for PcpA. First, 2,6-dihalophenols are not substrates but are able to bind to the active site as competitive inhibitors. Second, the heterosubstituted HQ, 2-Cl-6-MeHQ, binds in two different orientations leading to distinct products. Third, monosubstituted HQs are cleaved to an only limited extent by the enzyme but are potent inactivators.

The requirement for a *p*-hydroxyl group for ring cleavage can be readily explained by postulating that the first steps of the mechanism of PcpA (Scheme 4) are essentially the same as those of EDO. In the first step, substrate binds to the Fe(II) and is deprotonated to yield a monoanion. When O_2 binds, the *p*-hydroxyl group is deprotonated by an active site base, yielding an Fe(II)−superoxide−semiquinone ternary complex. The *p*-hydroxyl group is critical for stabilizing this ternary complex, promoting binding of the O_2 and its reduction to superoxide and yielding an electronic structure that promotes attack by O_2 on the aromatic ring. The one-electron oxidation of a phenolate would be far less favorable. Indeed, either an *o*/*p*-hydroxyl or an *o*-amino substituent that can conjugate to the ring is required for all ring-cleaving dioxygenases, except salicylate 1,2-dioxygenase (and even in that case, the rate of ring cleavage increases dramatically when a *p*-hydroxyl or amino group is present).[17,18] From this Fe(II)−superoxide−semiquinone ternary complex, attack by oxygen on the aromatic ring could occur at either the C1 or C2 position. We favor the former option. Formation of an alkylperoxide at C2 would necessitate that the rearrangement to the lactone proceed via an acyl migration, which is believed to be less favorable. Formation of an alkylperoxide at C1 would allow rearrangement to occur via an alkenyl migration, consistent with the EDO mechanism.

Bugg and co-workers have emphasized the importance of an alkenyl migration from the alkylperoxide intermediate to yield the observed extradiol cleavage in the EDOs, and that this is greatly favored over the alternative (an acyl migration to yield intradiol cleavage) because of both the orientation of the alkylperoxide and the presence of a proton donor in the second coordination sphere.[6] In PcpA, cleavage could occur between the hydroxyl group and either the *ortho* substituent proximal to the Fe(II) center (akin to an intradiol-type cleavage) or the substituent distal to the Fe(II) center (akin to an extradiol-type cleavage). However, with only one ligating hydroxyl group, the choice is not between an acyl or alkenyl migration, but instead between two different types of alkenyl migrations (proximal and distal). In the case of the symmetric substrates such as 2,6-diClHQ, because both alkenyl migrations would yield identical products, we cannot distinguish between these two options with the available data.

With 2-Cl-6-MeHQ, there are two potential explanations for how a mixture of products could arise. First, the substrate could bind to the active site in two orientations ("chloro-in" and "chloro-out") with only one type of alkenyl migration of the peroxide intermediate occurring; second, there could be only one binding mode for the substrate, and the two products form by partitioning between proximal and distal alkenyl migration. The second option is ruled out by the kinetic data, which show that the two ring-cleavage modes have different $K^{app}_{mO_2}$ values. As discussed above, a mechanism in which there is a single binding mode and a partitioning between products after that step does not yield such behavior. Neither the favored binding orientation nor the type of alkenyl migration is known; however, it is known that cleavage between the chloro and hydroxyl groups is preferred. Thus, either the substrate preferentially binds in the chloro-in conformation and the enzyme promotes a proximal alkenyl migration, or the substrate preferentially binds in the chloro-out conformation and the enzyme promotes a distal alkenyl migration. The minor product resulting from 1,6-cleavage would then arise from the other binding mode but the same type of alkenyl migration. Spectroscopic or structural studies that define the preferred binding orientation for an asymmetric substrate or inhibitor would thus define whether the mechanism of PcpA proceeds via a proximal or distal alkenyl migration.

Insights into the Mechanism of Inactivation in PcpA.

In PcpA, the monosubstituted HQs were substrates that strongly inactivate the enzyme, while for the *ortho*-disubstituted HQs, inactivation was at least 10-fold slower. Experiments in

Scheme 5. Plausible Mechanism for How a Monosubstituted Hydroquinone (ClHQ) Leads to Rapid Enzyme Inactivation with an Only Small Amount of Ring Cleavage

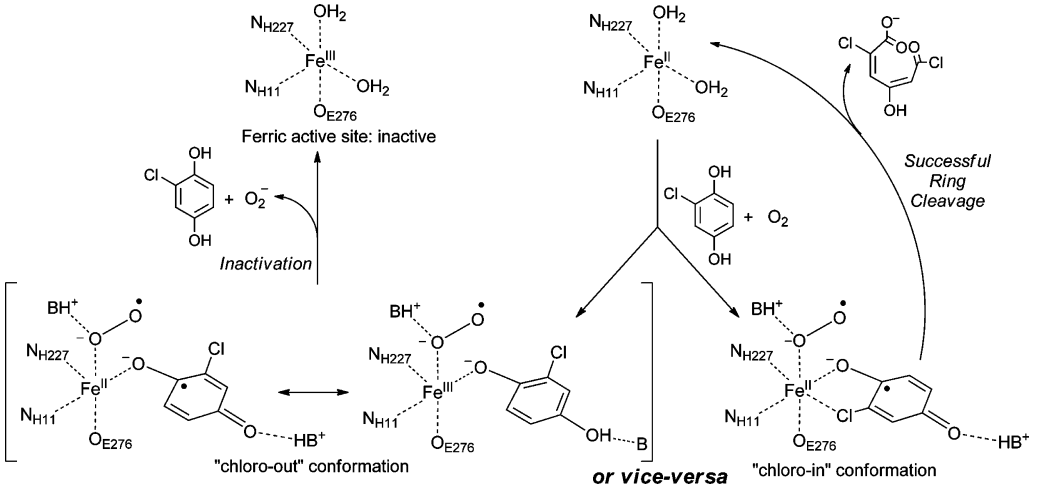

which PcpA was incubated with monosubstituted HQs in air-saturated versus O_2-free buffer indicate that inactivation is O_2-dependent, suggesting that oxidation of the Fe(II) center may be the source of the inactivation, as is known to be the case in the EDOs. Binding of O_2 to the monosubstituted HQ-bound Fe(II) center leads some ring cleavage and a significant amount of inactivation, whereas binding of O_2 to the disubsituted HQ-bound Fe(II) center leads to ring cleavage most of the time and inactivation only a small percentage of the time. Like 2-Cl-6-MeHQ, a monosubstituted HQ (such as ClHQ) can also bind in two different orientations: a chloro-in conformation in which the *o*-chloro substituent is near the Fe(II) center (and may weakly interact) and a chloro-out conformation in which the substituent is pointed away from the Fe(II) and interacts with some other part of the substrate binding pocket. One of the binding modes could lead to productive ring cleavage, while the other leads to efficient enzyme inactivation (Scheme 5). Which binding mode leads to inactivation cannot be determined with the available data, nor it is known what factors might cause ClHQ bound in a certain conformation to yield rapid enzyme inactivation.

The inhibitor 3-bromocatechol also inactivated the enzyme in an O_2-dependent fashion but did not lead to any detectable ring cleavage. The fact that 3-bromocatechol inactivates the enzyme but the *o*-dihalophenols do not highlights the importance of an *o*/*p*-hydroxyl group, which appears to be required for either ring cleavage or inactivation. Although inactivation with substrates has been reported in many EDOs, we are not aware of any studies of inactivation of EDOs with inhibitors.

CONCLUSION

Steady-state kinetic studies have demonstrated that PcpA has a high degree of substrate specificity: only 2,6-disubstituted HQs are efficiently oxidatively cleaved, while monosubstituted HQs show an only limited degree of ring cleavage but are potent inactivators of the enzyme. Likewise, 3-bromocatechol can bind and inactivate the enzyme but is not cleaved. This enzyme inactivation is O_2-dependent, suggesting that it may arise from irreversible oxidation of the Fe(II) center to an inactive Fe(III) state, as in known for the EDOs. A variety of 2,6-disubstituted phenols are good competitive inhibitors of PcpA. Both the trend in K_I among the inhibitors and the trend in the substrate specificity show a clear preference for halogen substituents at the *ortho* position over methyl substituents, with Br binding more tightly than Cl. A reason why catechols are not substrates for PcpA, despite the apparent similarity of the active site to that of the EDOs, can be partially established: most catechols bind (at best) weakly to the Fe(II) center, and those that bind reasonably well (3-bromocatechol) lead to rapid enzyme inactivation. These results, combined with the precedent of what is already known about the EDOs, allow several plausible features of the mechanism for PcpA to be proposed: (a) binding of the substrate as a monoanion and formation of a Fe(II)−superoxide−semiquinone ternary complex, (b) attack by O_2 at C1 to form an alkylperoxide intermediate, and (c) akenyl migration to form a lactone followed by its subsequent hydrolysis. The preferred mode of binding of asymmetric substrates cannot be determined with the available data. However, the preference for cleavage between the chloro and hydroxyl groups in the substrate 2-Cl-6-MeHQ can be combined with a future determination of substrate binding orientation to define whether a proximal or distal alkenyl migration is occurring. Future spectroscopic and structural studies will allow the determination of the basis for the unique specificity of PcpA.

ASSOCIATED CONTENT

Supporting Information

Derivation of the initial rate equations (eqs 4 and 5) for an asymmetric substrate binding to a single enzyme active site in two different orientations, EA and EA′, followed by a second substrate (O_2) yielding two different products, P and Q; a table of the ^{1}H NMR data of the cyclized form of the ring-cleavage products; a table of the relative initial rates of product formation upon incubation in air-saturated buffer with various compounds; and a figure showing the change in absorbance from product formation over time with substrate (2,6-diClHQ) and with varying concentrations of ClHQ or 2,6-dibromophenol. This material is available free of charge via the Internet at http://pubs.acs.org.

AUTHOR INFORMATION

Corresponding Author

*Phone: (509) 527-5799. Fax: (509) 527-5904. E-mail: machonte@whitman.edu.

Funding

This research was supported by grants from the American Chemical Society Petroleum Research Fund (ACS-PRF 44410-G3), the M. J. Murdock Charitable Trust, and the National Science Foundation (CHE-0951999), as well as funds from Whitman College. The purchase of the 400 MHz Bruker Avance III NMR spectrometer was supported by a grant from the National Science Foundation (MRI-0922775).

■ ACKNOWLEDGMENTS

We thank Prof. Marion Götz (Whitman College) for help on the synthesis, purification, and characterization of some of the substrates and reaction products and Prof. Jennifer Love (University of British Columbia, Vancouver, BC) and her students for use of their space and equipment for some of the syntheses. We thank Anees Daud (Whitman College) for synthesis of 2,6-dibromobenzoquinone. We thank Prof. Lindsay Eltis (University of British Columbia) for use of the O_2-sensitive electrode and other equipment, for advice on enzyme inactivation and derivation of rate equations, for other insightful discussions, and for a critical reading of the manuscript. We thank John Zimmerman (Whitman College) for preparation of some of the enzyme.

■ ABBREVIATIONS

BrHQ, bromohydroquinone; ClHQ, chlorohydroquinone; 2-Cl-6-MeHQ, 2-chloro-6-methylhydroquinone; DFT, density functional theory; 2,6-diBrHQ, 2,6-dibromohydroquinone; 2,6-diClHQ, 2,6-dichlorohydroquinone; 2,6-diMeHQ, 2,6-dimethylhydroquinone; DSS, sodium 3-(trimethylsilyl)-1-propanesulfonate; EDO, extradiol dioxygenase; HOHQ, hydroxyhydroquinone; HQDO, hydroquinone dioxygenase; HQs, hydroquinones; IDO, intradiol dioxygenase; MeHQ, methylhydroquinone; VOC, vicinal oxygenase chelate.

■ REFERENCES

(1) Furukawa, K. (2000) Engineering dioxygenases for efficient degradation of environmental pollutants. *Curr. Opin. Biotechnol. 11*, 244−249.

(2) Pieper, D. H., and Reineke, W. (2000) Engineering bacteria for bioremediation. *Curr. Opin. Biotechnol. 11*, 262−270.

(3) Pieper, D. H. (2005) Aerobic degradation of polychlorinated biphenyls. *Appl. Microbiol. Biotechnol. 67*, 170−191.

(4) Phillips, T. M., Seech, A. G., Lee, H., and Trevors, J. T. (2005) Biodegradation of hexachlorocyclohexane (HCH) by microorganisms. *Biodegradation 16*, 363−392.

(5) Stolz, A. (2009) Molecular characteristics of xenobiotic-degrading sphingomonads. *Appl. Microbiol. Biotechnol. 81*, 793−811.

(6) Bugg, T. D. H., and Lin, G. (2001) Solving the riddle of the intradiol and extradiol catechol dioxygenases: How do enzymes control hydroperoxide rearrangements? *Chem. Commun.*, 941−952.

(7) Bugg, T. D. H. (2003) Dioxygenase enzymes: Catalytic mechanisms and chemical models. *Tetrahedron 59*, 7075−7101.

(8) Vaillancourt, F. H., Bolin, J. T., and Eltis, L. (2004) Ring-Cleavage Dioxygenase. In *Pseudomonas* (Ramos, J.-L., Ed.) pp 359−396, Kluwer Academic/Plenum, New York.

(9) Vaillancourt, F. H., Bolin, J. T., and Eltis, L. D. (2006) The ins and outs of ring-cleaving dioxygenases. *Crit. Rev. Biochem. Mol. Biol. 41*, 241−267.

(10) Bugg, T. D. H., and Ramaswamy, S. (2008) Non-heme iron-dependent dioxygenases: Unravelling catalytic mechanisms for complex enzymatic oxidations. *Curr. Opin. Chem. Biol. 12*, 134−140.

(11) Kovaleva, E. G., and Lipscomb, J. D. (2007) Crystal structures of Fe^{2+} dioxygenase superoxo, alkylperoxo, and bound product intermediates. *Science 316*, 453−457.

(12) Kovaleva, E. G., and Lipscomb, J. D. (2008) Intermediate in the O-O Bond Cleavage Reaction of an Extradiol Dioxygenase. *Biochemistry 47*, 11168−11170.

(13) Deeth, R. J., and Bugg, T. D. H. (2003) A density functional investigation of the extradiol cleavage mechanism in non-heme iron catechol dioxygenase. *J. Biol. Inorg. Chem. 8*, 409−418.

(14) Siegbahn, P. E. M., and Haeffner, F. (2004) Mechanism for Catechol Ring-Cleavage by Non-Heme Iron Extradiol Dioxygenase. *J. Am. Chem. Soc. 126*, 8919−8932.

(15) Harpel, M. R., and Lipscomb, J. D. (1990) Gentisate 1,2-Dioxygenase from *Pseudomonas*. Purification, Characterization, and Comparison of the Enzymes from *Pseudomonas testosteroni* and *Pseudomonas acidovorans*. *J. Biol. Chem. 265*, 6301−6311.

(16) Harpel, M. R., and Lipscomb, J. D. (1990) Gentisate 1,2-Dioxygenase from *Pseudomonas*. Substrate Coordination to Active-Site Fe^{2+} and Mechanism of Turnover. *J. Biol. Chem. 265*, 22187−22196.

(17) Hintner, J.-P., Lechner, C., Rigert, U., Kuhm, A. E., Storm, T., Reemtsma, T., and Stolz, A. (2001) Direct Ring Fission of Salicylate by a Salicylate 1,2-Dioxygenase Activity from *Pseudaminobacter salicylatoxidans*. *J. Bacteriol. 183*, 6936−6942.

(18) Hintner, J.-P., Remtsma, T., and Stolz, A. (2004) Biochemical and molecular characterization of a ring fission dioxygenase with the ability to oxidize (substituted) salicylate(s) from *Pseudaminobacter salicylatoxidans*. *J. Biol. Chem. 279*, 37250−37260.

(19) Adams, M. A., Singh, V. K., Keller, B. O., and Jia, Z. C. (2006) Structural and biochemical characterization of gentisate 1,2-dioxygenase from *Escherichia coli* O157: H7. *Mol. Microbiol. 61*, 1469−1484.

(20) Chen, J., Li, W., Wang, M. Z., Zhu, G. Y., Liu, D. Q., Sun, F., Hao, N., Li, X. M., Rao, Z. H., and Zhang, X. C. (2008) Crystal structure and mutagenic analysis of GDOsp, a gentisate 1,2-dioxygenase from *Silicibacter pomeroyi*. *Protein Sci. 17*, 1362−1373.

(21) Matera, I., Ferraroni, M., Burger, S., Scozzafava, A., Stolz, A., and Briganti, F. (2008) Salicylate 1,2-dioxygenase from *Pseudaminobacter salicylatoxidans*: Crystal structure of a peculiar ring-cleaving dioxygenase. *J. Mol. Biol. 380*, 856−868.

(22) Titus, G. P., Mueller, H. A., Burgner, J., Rodríguez-de-Córba, S., Peñalva, M. A., and Timm, D. E. (2000) Crystal structure of human homogentisate dioxygenase. *Nat. Struct. Biol. 7*, 542−546.

(23) Veldhuizen, E. J. A., Vaillancourt, F. H., Whiting, C. J., Hsiao, M. M. Y., Gingras, G., Xiao, Y. F., Tanguay, R. M., Boukouvalas, J., and Eltis, L. D. (2005) Steady-state kinetics and inhibition of anaerobically purified human homogentisate 1,2-dioxygenase. *Biochem. J. 386*, 305−314.

(24) Malherbe, P., Kohler, C., Daprada, M., Lang, G., Kiefer, V., Schwarcz, R., Lahm, H. W., and Cesura, A. M. (1994) Molecular-Cloning and Functional Expression of Human 3-Hydroxyanthranilic-Acid Dioxygenase. *J. Biol. Chem. 269*, 13792−13797.

(25) Lendenmann, U., and Spain, J. C. (1996) 2-Aminophenol 1,6-Dioxygenase: A Novel Aromatic Ring Cleavage Enzyme Purified from *Pseudomonas pseudoalcaligenes* JS45. *J. Bacteriol. 178*, 6227−6232.

(26) Davis, J. K., He, Z., Somerville, C. C., and Spain, J. C. (1999) Genetic and biochemical comparison of 2-aminophenol 1,6-dixygenase of *Pseudomonas pseudoalcaligenes* JS45 to meta-cleavage dioxygenases: Divergent evolution of 2-aminophenol meta-cleavage pathway. *Arch. Microbiol. 172*, 330−339.

(27) Zhang, Y., Colabroy, K. L., Begley, T. P., and Ealick, S. E. (2005) Structural studies on 3-hydroxyanthranilate-3,4-dioxygenase: The catalytic mechanism of a complex oxidation involved in NAD biosynthesis. *Biochemistry 44*, 7632−7643.

(28) Ohtsubo, Y., Miyauchi, K., Kanda, K., Hatta, T., Kiyohara, H., Senda, T., Nagata, Y., Mitsui, Y., and Takagi, M. (1999) PcpA, which is involved in the degradation of pentachlorophenol in *Sphingomonas chlorophenolica* ATCC39723, is a novel type of ring-cleavage dioxygenase. *FEBS Lett. 459*, 395−398.

(29) Xu, L., Resing, K., Lawson, S. L., Babbitt, P. C., and Copley, S. D. (1999) Evidence That *pcpA* Encodes 2,6-Dichlorohydroquinone Dioxygenase, the Ring Cleavage Enzyme Required for Pentachlorophenol Degradation in *Sphingomonas chlorophenolica* Strain ATCC 39723. *Biochemistry 38*, 7659−7669.

(30) Xun, L., Bohuslavek, J., and Cai, M. (1999) Characterization of 2,6-Dichloro-*p*-hydroquinone 1,2-Dioxygenase (PcpA) of *Sphingomonas chlorophenolica* ATCC 39723. *Biochem. Biophys. Res. Commun. 266*, 322−325.

(31) Miyauchi, K., Adachi, Y., Nagata, Y., and Takagi, M. (1999) Cloning and Sequencing of a Novel *meta*-Clevage Dioxygenase Gene Whose Product Is Involved in Degradation of γ-Hexachlorocyclohexane in *Sphingomonas paucimobilis*. *J. Bacteriol. 181*, 6712−6719.

(32) Moonen, M. J. H., Synowsky, S. A., van den Berg, W. A. M., Westphal, A. H., Heck, A. J. R., van den Heuvel, R. H. H., Fraaije, M. W., and van Berkel, W. J. H. (2008) Hydroquinone dioxygenase from *Pseudomonas fluorescens* ACB: A novel member of the family of nonheme-iron(II)-dependent dioxygenases. *J. Bacteriol. 190*, 5199−5209.

(33) Shen, W. J., Liu, W. D., Zhang, J., Tao, J. A., Deng, H. H., Cao, H., and Cui, Z. L. (2010) Cloning and characterization of a gene cluster involved in the catabolism of *p*-nitrophenol from *Pseudomonas putida* DLL-E4. *Bioresour. Technol. 101*, 7516−7522.

(34) Yin, Y., and Zhou, N. Y. (2010) Characterization of MnpC, a Hydroquinone Dioxygenase Likely Involved in the *meta*-Nitrophenol Degradation by *Cupriavidus necator* JMP134. *Curr. Microbiol. 61*, 471−476.

(35) Machonkin, T. E., Holland, P. L., Smith, K. N., Liberman, J. S., Dinescu, A., Cundari, T. R., and Rocks, S. S. (2010) Determination of the Active Site of *Sphingobium chlorophenolicum* 2,6-dichlorohydroquinone dioxygenase (PcpA). *J. Biol. Inorg. Chem. 10*, 291−301.

(36) Bartels, I., Knackmuss, H.-J., and Reineke, W. (1984) Suicide Inactivation of Catechol 2,3-Dioxygenase from *Pseudomonas putida* mt-2 by 3-Halocatechols. *Appl. Environ. Microbiol. 47*, 500−505.

(37) Cerdan, P., Wasserfallen, A., Rekik, M., Timmis, K. N., and Harayama, S. (1994) Substrate Specificity of Catechol 2,3-Dioxygenase Encoded by TOL Plasmid pWW0 of *Pseudomonas putida* and Its Relationship to Cell Growth. *J. Bacteriol. 176*, 6074−6081.

(38) Vaillancourt, F. H., Labbé, G., Drouin, N. M., Fortin, P. D., and Eltis, L. D. (2002) The Mechanism-based Inactivation of 2,3-Dihydroxybiphenyl 1,2-Dioxygenase by Catecholic Substrates. *J. Biol. Chem. 277*, 2019−2027.

(39) Dai, S., Vaillancourt, F. H., Maaroufi, H., Drouin, N. M., Neau, D. B., Snieckus, V., Bolin, J. T., and Eltis, L. D. (2002) Identification and analysis of a bottleneck in PCB biodegradation. *Nat. Struct. Biol. 9*, 934−939.

(40) Mars, A. E., Kasberg, T., Kaschabek, S. R., vanAgteren, M. H., Janssen, D. B., and Reineke, W. (1997) Microbial Degradation of Chloroaromatics: Use of the *meta*-Cleavage Pathway for Mineralization of Chlorobenzene. *J. Bacteriol. 179*, 4530−4537.

(41) Kaschabek, S. R., Kasberg, T., Müller, D., Mars, A. E., Janssen, D. B., and Reineke, W. (1998) Degradation of Chloroaromatics: Purification and Characterization of a Novel Type of Chlorocatechol 2,3-Dioxygenase of *Pseudomonas putida* GJ31. *J. Bacteriol. 180*, 296−302.

(42) Riegert, U., Heiss, G., Fischer, P., and Stolz, A. (1998) Distal Cleavage of 3-Chlorocatechol by an Extradiol Dioxygenase to 3-Chloro-2-Hydroxymuconic Semialdehyde. *J. Bacteriol. 180*, 2849−2853.

(43) Mars, A. E., Kingma, J., Kaschabek, S. R., Reineke, W., and Janssen, D. (1999) Conversion of 3-Chlorocatechol by Various Catechol 2,3-Dioxygenases and Sequence Analysis of the Chlorocatechol Dioxygenase Region of *Pseudomonas putida* GJ31. *J. Bacteriol. 181*, 1309−1318.

(44) Riegert, U., Heiss, G., Kuhn, A. E., Müller, C., Contzen, M., Knackmuss, H.-J., and Stolz, A. (1999) Catalytic Properties of the 3-Chlorocatechol-Oxidizing 2,3-Dihydroxybiphenyl 1,2-Dioxygenase from *Sphingomonas* sp. Strain BN6. *J. Bacteriol. 181*, 4812−4817.

(45) Vaillancourt, F. H., Haro, M. A., Drouin, N. M., Karim, Z., Maaroufi, H., and Eltis, L. D. (2003) Characterization of extradiol dioxygenases from a polychlorinated biphenyl-degrading strain that possess higher specificities for chlorinated metabolites. *J. Bacteriol. 185*, 1253−1260.

(46) Fortin, P. D., Lo, A. T.-F., Haro, M.-A., Kaschabek, S. R., Reineke, W., and Eltis, L. D. (2005) Evolutionarily Divergent Extradiol Dioxygenases Possess Higher Specificities for Polychlorinated Biphenyl Metabolites. *J. Bacteriol. 187*, 415−421.

(47) Riegert, U., Bürger, S., and Stolz, A. (2001) Altering Catalytic Properties of 3-Chlorocatechol-Oxidizing Extradiol Dioxygenase from *Sphingomonas xenophaga* BN6 by Random Mutagenesis. *J. Bacteriol. 183*, 2322−2330.

(48) Ohnishi, K., Okuta, A., Ju, J. S., Hamada, T., Misono, H., and Harayama, S. (2004) Molecular breeding of 2,3-dihydroxybiphenyl 1,2-dioxygenase for enhanced resistance to 3-chlorocatechol. *J. Biochem. 135*, 305−317.

(49) Okuta, A., Ohnishi, K., and Harayama, S. (2004) Construction of chimeric catechol 2,3-dioxygenase exhibiting improved activity against the suicide inhibitor 4-methylcatechol. *Appl. Environ. Microbiol. 70*, 1804−1810.

(50) Fortin, P. D., MacPherson, I., Neau, D. B., Bolin, J. T., and Eltis, L. D. (2005) Directed evolution of a ring-cleaving dioxygenase for polychlorinated biphenyl degradation. *J. Biol. Chem. 280*, 42307−42314.

(51) Ungnade, H. E., and Zilch, K. T. (1951) Phenoxyquinones. II. The Diphenoxyquinones. *J. Org. Chem. 16*, 64−69.

(52) Burton, H., and Prail, P. F. G. (1952) Acylation Reactions Catalyzed by Strong Acids. Part VI. A Comparison of Zinc Chloride and Perchloric Acid as Catalysts for the Thiele Acetylation of Quinones. *J. Chem. Soc.*,, 755−759.

(53) Harris, D. C. (1998) Nonlinear least-squares curve fitting with Microsoft excel solver. *J. Chem. Educ. 75*, 119−121.

(54) Kaschabek, S. R., and Reineke, W. (1992) Maleylacetate Reductase of *Pseudomonas* Sp Strain B13: Dechlorination of Chloromaleylacetates, Metabolites in the Degradation of Chloroaromatic Compounds. *Arch. Microbiol. 158*, 412−417.

(55) Fowler, J., and Seltzer, S. (1970) Synthesis of Model Compounds for Maleylacetoacetic Acid. Maleylacetone. *J. Org. Chem. 35*, 3529−3532.

(56) Prucha, M., Wray, V., and Pieper, D. H. (1996) Metabolism of 5-chlorosubstituted muconolactones. *Eur. J. Biochem. 237*, 357−366.

(57) Pieper, D. H., Pollmann, K., Nikodem, P., Gonzalez, B., and Wray, V. (2002) Monitoring key reactions in degradation of chloroaromatics by *in situ* H-1 nuclear magnetic resonance: Solution structures of metabolites formed from *cis*-dienelactone. *J. Bacteriol. 184*, 1466−1470.

(58) Seltzer, S. (1981) Nuclear Magnetic Resonance, Paramagnetic Ion Induced Relaxation Method to Differentiate between 1,3-Diketo and 1,3-Keto-Enol Isomers. *J. Org. Chem. 46*, 2643−2650.

(59) Cain, R. B., Fortnagel, P., Hebenbrock, S., Kirby, G. W., McLenaghan, H. J. S., Rao, G. V., and Schmidt, S. (1997) Biosynthesis of a cyclic tautomer of (3-methylmaleyl)acetone from 4-hydroxy-3,5-dimethylbenzoate by *Pseudomonas* sp. HH35 but not by *Rhodococcus rhodochrous* N75. *Biochem. Biophys. Res. Commun. 238*, 197−201.

(60) Schmidt, S., and Kirby, G. W. (2001) Dioxygenative cleavage of C-methylated hydroquinones and 2,6-dichlorohydroquinone by *Pseudomonas* sp HH35. *Biochim. Biophys. Acta 1568*, 83−89.

(61) Silverstein, R. M., Bassler, G. C., and Morrill, T. C. (1991) *Spectrometric Identification of Organic Compounds*, 5th ed., Wiley, New York.

(62) Fujiwara, M., Golovleva, L. A., Saeki, Y., Nozaki, M., and Hayaishi, O. (1975) Extradiol Cleavage of 3-Substituted Catechols by an Intradiol Dioxygenase, Pyrocatechase, from a Pseudomonad. *J. Biol. Chem. 250*, 4848−4855.

(63) Cornish-Bowden, A. (2004) *Fundamentals of Enzyme Kinetics*, 3rd ed., Portland Press, London.

(64) Borowski, T., Georgiev, V., and Siegbahn, P. E. M. (2005) Catalytic reaction mechanism of homogentisate dioxygenase: A hybrid DFT study. *J. Am. Chem. Soc. 127*, 17303−17314.

(65) Auffinger, P., Hays, F. A., Westhof, E., and Ho, P. S. (2004) Halogen bonds in biological molecules. *Proc. Natl. Acad. Sci. U.S.A. 101*, 16789−16794.

(66) Imai, Y. N., Inoue, Y., Nakanishi, I., and Kitaura, K. (2008) Cl-π interactions in protein-ligand complexes. *Protein Sci. 17*, 1129−1137.
(67) Lommerse, J. P. M., Stone, A. J., Taylor, R., and Allen, F. H. (1996) The nature and geometry of intermolecular interactions between halogens and oxygen or nitrogen. *J. Am. Chem. Soc. 118*, 3108−3116.
(68) Matter, H., Nazare, M., Gussregen, S., Will, D. W., Schreuder, H., Bauer, A., Urmann, M., Ritter, K., Wagner, M., and Wehner, V. (2009) Evidence for C-Cl/C-Br$\cdots\pi$ Interactions as an Important Contribution to Protein-Ligand Binding Affinity. *Angew. Chem., Int. Ed. 48*, 2911−2916.
(69) Metrangolo, P., Meyer, F., Pilati, T., Resnati, G., and Terraneo, G. (2008) Mutual induced coordination in halogen-bonded anionic assemblies with (6,3) cation-templated topologies. *Chem. Commun.*, 1635−1637.
(70) Kulawiec, R. J., and Crabtree, R. H. (1990) Coordination Chemistry of Halocarbons. *Coord. Chem. Rev. 99*, 89−115.
(71) Wulfsberg, G., Yanisch, J., Meyer, R., Bowers, J., and Essig, M. (1984) Lewis-Base Properties of *Ortho* Chlorines in Copper(II) 2,4,6-Trichlorophenolates, 4-Bromo-2,6-Dichlorophenolates, and 2,6-Dichlorophenolates as Studied by Cl-35 Nuclear-Quadrupole Resonance Spectroscopy. *Inorg. Chem. 23*, 715−719.
(72) Richardson, M. F., Wulfsberg, G., Marlow, R., Zaghonni, S., McCorkle, D., Shadid, K., Gagliardi, J. Jr., and Farris, B. (1993) Coordination of ortho chlorines in nickel and zinc 4-substituted 2,6-dichlorophenolates. Crystal and molecular structures of (N,N,N′,N′-tetramethyl-1,2-ethanediamine)bis(2,4,6-trichlorophenolato-O,Cl)-nickel(II) and tris(pyridine)bis(2,4,6-trichlorophenolato-O)nickel(II). *Inorg. Chem. 32*, 1913−1919.
(73) Rocks, S. S., Brennessel, W. W., Machonkin, T. E., and Holland, P. L. (2010) Solution and Structural Characterization of Iron(II) Complexes with *Ortho*-Halogenated Phenolates: Insights Into Potential Substrate Binding Modes in Hydroquinone Dioxygenases. *Inorg. Chem. 49*, 10914−10929.
(74) Arciero, D. M., Orville, A. M., and Lipscomb, J. D. (1985) [^{17}O]Water and Nitric Oxide Binding by Protocatechuate 4,5-Dioxygenase and Catechol 2,3-Dioxygenase. *J. Biol. Chem. 260*, 14035−14044.
(75) Bertini, I., Briganti, F., and Scozzafava, A. (1994) Aliphatic and Aromatic Inhibitors Binding to the Active-Site of Catechol 2,3-Dioxygenase from *Pseudomonas putida* mt-2. *FEBS Lett. 343*, 56−60.
(76) Kobayashi, T., Ishida, T., Horiike, K., Takahara, Y., Numao, N., Nakazawa, A., Nakazawa, T., and Nozaki, M. (1995) Overexpression of *Pseudomonas putida* Catechol 2,3-Dioxygenase with High Specific Activity by Genetically-Engineered *Escherichia coli*. *J. Biochem. 117*, 614−622.